Neutrino mass and invisible Higgs decays at the LHC

Cesar Bonilla,[1,*] Jorge C. Romão,[2,†] and José W. F. Valle[1,‡]

[1]*AHEP Group, Instituto de Física Corpuscular-C.S.I.C./Universitat de València Edificio de Institutos de Paterna, C/Catedratico José Beltrán, 2 E-46980 Paterna (València), Spain*
[2]*Departamento de Física and CFTP, Instituto Superior Técnico Universidade de Lisboa, Av. Rovisco Pais 1, 1049-001 Lisboa, Portugal*

The discovery of the Higgs boson suggests that neutrinos also get their mass from spontaneous symmetry breaking. In the simplest ungauged lepton-number scheme, the Standard Model Higgs now has two other partners: a massive *CP*-even scalar, and the massless Nambu-Goldstone boson, called the Majoron. For weak-scale breaking of lepton number the invisible decays of the *CP*-even Higgs bosons to the Majoron lead to potentially copious sources of events with large missing energy. Using LHC results, we study how the constraints on invisible decays of the Higgs boson restrict the relevant parameters, substantially extending those previously derived from LEP and potentially shedding light on the scale of spontaneous lepton-number violation.

I. INTRODUCTION

The recently discovered Standard Model (SM) Higgs boson is most likely the first of a family. Indeed, after the historic Higgs discovery by the LHC experiments [1,2] it is more than ever natural to imagine that the Brout-Englert-Higgs (BEH) mechanism [3–5] is also responsible for generating all masses in particle physics, including those of neutrinos [6]. Extra Higgs scalars are also expected in order to account for the existing cosmological puzzles, such as dark matter and inflation, as well as to realize natural schemes of symmetry breaking, such as those based on supersymmetry.

Here we focus on neutrino masses. These are expected to arise from the exchange of some heavy messenger states which, depending on the underlying mechanism, need not be too heavy [7,8]. If lepton number is broken through an $\mathrm{SU}(3)_c \otimes \mathrm{SU}(2)_L \otimes \mathrm{U}(1)_Y$ singlet vacuum expectation value [9,10] there is a physical pseudoscalar Nambu-Goldstone boson—the Majoron. All Majoron couplings to SM particles are very small except, perhaps, those with the Higgs boson. As a result the *CP*-even Higgs scalars have sizable "invisible" decays, for example [8,11,12],

$$h \rightarrow JJ, \qquad (1)$$

where $J \equiv \sqrt{2}\mathrm{Im}\sigma$ denotes the associated pseudoscalar Goldstone boson—the Majoron. The coexistence of such novel decays with the SM decay modes affects the Higgs mass bounds obtained [13–16] and provides new clues to the ongoing Higgs boson searches at the LHC.

Current LHC data suggest that the new particle discovered with a mass $m = 125$ GeV [1,2] is indeed the long-awaited

SM Higgs boson ($m_H = m$). This places restrictions on the extended Higgs sector providing neutrino masses, which we now analyze. We find that, despite the data accumulated so far at the LHC, the possibility of having an invisibly decaying Higgs boson is not too tightly constrained. Experimental searches have been mainly motivated by dark matter models where the Higgs might decay into the dark matter candidate, say χ, if its mass is $m_\chi < \frac{m_H}{2}$, such as supersymmetric models with *R*-parity conservation. However, invisible Higgs boson decays appear most naturally in low-scale models of neutrino mass generation. In these models neutrino masses arise from the spontaneous breaking of an additional U(1) global symmetry associated to lepton number in the $\mathrm{SU}(3)_c \otimes \mathrm{SU}(2)_L \otimes \mathrm{U}(1)_Y$ theory. This symmetry is broken when a lepton-number-carrying scalar singlet σ gets a nonzero vacuum expectation value (VEV), i.e., $\langle\sigma\rangle = v_1$.

There are many genuine low-scale neutrino mass scenarios of this type [7], such as inverse [17,18] or linear 21–19]] seesaw schemes. For simplicity, however, one may take the simplest $\mathrm{SU}(3)_c \otimes \mathrm{SU}(2)_L \otimes \mathrm{U}(1)_Y$ extension of neutrino mass generation, namely the type-I seesaw mechanism [22–26]. In this case, in order to account for the small neutrino masses one must assume very small Dirac-type Yukawa couplings. The important consequence of spontaneous breaking of lepton number is the appearance of a physical Goldstone boson [9,10] and the decays in Eq. (1). The scalar sector, in the simplest scenario, contains only one SU(2) scalar doublet ϕ and a singlet σ, which was called the 12-model in Ref. [10]. Hence there are three physical spin-zero states: the two massive *CP*-even scalars H_1 and H_2, and one massless pseudoscalar, the Majoron J. Assuming the ordering $m_{H_1} < m_{H_2}$, the most interesting case is when $m_{H_2} = 125$ GeV. In this paper we focus on the possibility that the Higgs H_2 is the one reported by the

*[*]cesar.bonilla@ific.uv.es
[†]jorge.romao@tecnico.ulisboa.pt
[‡]valle@ific.uv.es

LHC,[1] i.e., $m_{H_2} = 125$ GeV, and that in general the *CP*-even scalars can decay into Majorons as follows:

$$H_i \to JJ \quad \text{and} \quad H_2 \to 2H_1 \to 4J$$

$$\left(\text{when } m_{H_1} < \frac{m_{H_2}}{2} \right). \tag{2}$$

We note that there are strong constraints on invisible decays of a scalar with a mass below ~115 GeV coming from the searches carried out by LEP [15]. In the next section we describe the main features of the symmetry-breaking sector of the 12-model. We present our results in Sec. III, and we discuss how the main features of this simplest model can also be present in other schemes with additional experimental signatures in Sec. IV. We conclude in Sec. V.

II. SYMMETRY BREAKING IN THE 12-MODEL

The simplest way to model spontaneous lepton-number violation contains, in addition to the usual SM Higgs doublet ϕ,

$$\phi = \begin{bmatrix} \phi^0 \\ \phi^- \end{bmatrix}, \tag{3}$$

a complex lepton-number-carrying scalar singlet σ that acquires a nonzero VEV $\langle \sigma \rangle$ that breaks the global $U(1)_L$ symmetry [9,10]. This scalar gives Majorana mass to right-handed neutrinos, while ϕ couples to SM fermions. This structure defines the simplest type-I seesaw scheme with spontaneous symmetry breaking. Many other scenarios sharing the same symmetry-breaking sector can be envisaged though, for definiteness, we assume the simplest type-I seesaw.

A. The scalar potential

The scalar potential is given by [8,11,12]

$$V = \mu_1^2 \sigma^\dagger \sigma + \mu_2^2 \phi^\dagger \phi + \lambda_1 (\sigma^\dagger \sigma)^2 + \lambda_2 (\phi^\dagger \phi)^2$$

$$+ \lambda_{12} (\sigma^\dagger \sigma)(\phi^\dagger \phi). \tag{4}$$

The singlet σ and the neutral component of the doublet ϕ acquire vacuum expectation values v_1 and v_2, respectively. Therefore we shift the fields as

$$\sigma = \frac{v_1}{\sqrt{2}} + \frac{R_1 + iI_1}{\sqrt{2}}, \quad \phi^0 = \frac{v_2}{\sqrt{2}} + \frac{R_2 + iI_2}{\sqrt{2}}. \tag{5}$$

Solving the minimization equations, we can obtain μ_1^2 and μ_2^2 as functions of the VEVs in the usual way,

---

$$\mu_1^2 = -\lambda_1 v_1^2 - \frac{1}{2}\lambda_{12} v_2^2,$$

$$\mu_2^2 = -\lambda_2 v_2^2 - \frac{1}{2}\lambda_{12} v_1^2. \tag{6}$$

B. Neutral Higgs mass matrices

By evaluating the second derivatives of the scalar potential at the minimum one finds—in the basis (R_1, R_2) and (I_1, I_2)—the *CP*-even and *CP*-odd mass matrices, M_R^2 and M_I^2,

$$M_R^2 = \begin{bmatrix} 2\lambda_1 v_1^2 & \lambda_{12} v_1 v_2 \\ \lambda_{12} v_1 v_2 & 2\lambda_2 v_2^2 \end{bmatrix}, \qquad M_I^2 = \begin{bmatrix} 0 & 0 \\ 0 & 0 \end{bmatrix}. \tag{7}$$

As expected, the *CP*-odd mass matrix has two zero eigenvalues. One corresponds to the would-be Goldstone boson which becomes the longitudinal component of the Z boson after the BEH mechanism. The other is the physical Goldstone boson resulting from the breaking of the global symmetry, namely the Majoron J. Hence we have

$$J = I_1, \qquad G^0 = I_2. \tag{8}$$

For the *CP*-even Higgs bosons we define the two mass eigenstates H_i through the rotation matrix O_R as

$$\begin{bmatrix} H_1 \\ H_2 \end{bmatrix} = O_R \begin{bmatrix} R_1 \\ R_2 \end{bmatrix} \equiv \begin{bmatrix} \cos\alpha & \sin\alpha \\ -\sin\alpha & \cos\alpha \end{bmatrix} \begin{bmatrix} R_1 \\ R_2 \end{bmatrix}, \tag{9}$$

satisfying

$$O_R M_R^2 O_R^T = \text{diag}(m_{H_1}^2, m_{H_2}^2). \tag{10}$$

One can use Eqs. (10) and (7) in order to solve for the parameters λ_1, λ_2, and λ_{12} in terms of the two physical masses and the mixing angle α. We get

$$\lambda_1 = \frac{m_{H_1}^2 \cos^2\alpha + m_{H_2}^2 \sin^2\alpha}{2v_1^2},$$

$$\lambda_2 = \frac{m_{H_1}^2 \sin^2\alpha + m_{H_2}^2 \cos^2\alpha}{2v_2^2},$$

$$\lambda_{12} = \frac{\sin\alpha \cos\alpha (m_{H_1}^2 - m_{H_2}^2)}{v_1 v_2}. \tag{11}$$

C. Higgs couplings and decay widths

The couplings of the Higgs boson to Standard Model particles get modified according to the substitution rule

$$h \to \sin\alpha H_1 + \cos\alpha H_2. \tag{12}$$

In addition to these, there are two new important couplings coming from the extended Higgs sector, namely $H_2H_1H_1$ and H_iJJ. The former is given, with our conventions[2], by

$$g_{H_2H_1H_1} = 2v\left[3\lambda_2\cos\alpha\sin\alpha^2 - 3\lambda_1\cos\alpha^2\sin\alpha\cot\beta\right.$$
$$\left. - \frac{\lambda_{12}}{8}\csc\beta(\sin(\alpha-\beta) - 3\sin(3\alpha+\beta))\right], \quad (13)$$

or in terms of the masses,

$$g_{H_2H_1H_1} = \frac{1}{2v_1v_2}(2m_{H_1}^2 + m_{H_2}^2)\sin 2\alpha(\sin\alpha v_1 - \cos\alpha v_2)$$
$$= \frac{\tan\beta}{2v}(2m_{H_1}^2 + m_{H_2}^2)\sin 2\alpha(\cot\beta\sin\alpha - \cos\alpha),$$

while the couplings H_iJJ are given by

$$g_{H_iJJ} = \frac{\tan\beta}{v}m_{H_i}^2 O_{Ri1}, \quad (14)$$

where we have defined

$$v = v_2 = \frac{2m_W}{g}, \qquad \tan\beta = \frac{v_2}{v_1}, \quad (15)$$

which are responsible for the invisible Higgs decays. The decay widths to SM states are obtained from those of the SM with the help of the substitution rule in Eq. (12). On the other hand, the new widths leading to the invisible Higgs boson decays are

$$H_2 \to H_1H_1 \quad \text{and} \quad H_i \to JJ, \quad (16)$$

which are given by

$$\Gamma(H_2 \to H_1H_1) = \frac{g_{H_2H_1H_1}^2}{32\pi m_{H_2}}\left(1 - \frac{4m_{H_1}^2}{m_{H_2}^2}\right)^{1/2} \quad (17)$$

and

$$\Gamma(H_i \to JJ) = \frac{1}{32\pi}\frac{g_{H_iJJ}^2}{m_{H_i}}. \quad (18)$$

III. RESULTS

We now discuss the constraints on invisibly decaying Higgs bosons which follow from searches performed at LEP as well as the LHC. We focus on the case where the Higgs H_2 is the one reported by the LHC, i.e., $m_{H_2} = 125$ GeV, while $m_{H_1} < m_{H_2}$. Both states may in

---

[2]Our Higgs trilinear self-coupling parameters are obtained after minimizing the Higgs potential. In order to get the Feynman rules we have to multiply by $-i$.

principle have SM-like as well as invisible decays to Majorons, as given in Eq. (2).

A. Parameter sampling procedure

In order to cover the possibility of a Higgs boson with a mass below 125 GeV, we generate points in parameter space taking $m_{H_2} = 125$ GeV and $15 < m_{H_1} < 115$ GeV. In our simple model, the only remaining parameters are the VEV v_1 characterizing the spontaneous violation of lepton number and the mixing angle α, which we take as

$$v_1 \in [500, 1500]\ \text{GeV}, \qquad \alpha \in [0, \pi]. \quad (19)$$

However, as the results do not depend very much on the value of v_1 in that interval, we will use $v_1 = 1000$ GeV in most of the results presented.

B. Theoretical constraints

The points generated must fulfill several constraints. The first are the consistency requirements for the scalar potential, namely that it must be bounded from below and that perturbative unitarity is respected. The unbounded-from-below constraint reads [29]

$$\lambda_1 > 0, \qquad \lambda_2 > 0, \qquad \lambda_{12} + 2\sqrt{\lambda_1\lambda_2} > 0, \quad (20)$$

while for unitarity we just take a simplified approach requiring that all couplings are less than $\sqrt{4\pi}$. Certainly this can be refined [30], though Eq. (20) is sufficient for our current purposes.

C. Constraints from invisible decay searches

The second type of constraints come from the LEP collider. Searches for invisibly decaying Higgs bosons using the LEP-II data have been performed by the LEP collaborations. In our setup these constraints apply to the lightest Higgs boson, H_1. For the channel $e^+e^- \to ZH \to Zb\bar{b}$ the final state is expressed in terms of the SM HZ cross section through

$$\sigma_{hZ\to b\bar{b}Z} = \sigma_{HZ}^{SM} \times R_{HZ} \times \text{BR}(H \to b\bar{b})$$
$$= \sigma_{HZ}^{SM} \times C_{Z(H\to b\bar{b})}^2, \quad (21)$$

where R_{HZ} is the suppression factor related to the coupling of the Higgs boson to the gauge boson Z (i.e., $R_{hZ}^{SM} = 1$ and for the model we have $R_{H_1Z} = \sin^2\alpha$; note also that $C_{Z(H\to b\bar{b})}^2$ is independent of m_H). Here $\text{BR}(H \to b\bar{b})$ is the branching ratio (BR) of the channel $H \to b\bar{b}$, which in the model is modified with respect to the SM by the presence of the invisible Higgs boson decay into the Goldstone boson J associated to the breaking of the global $U(1)_L$ symmetry.
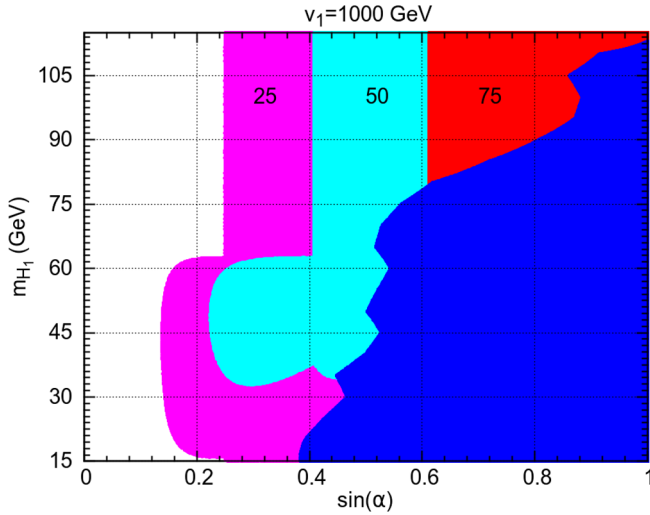
FIG. 1 (color online). m_{H_1} versus $\sin\alpha$ in the model for $v_1 = 1000$ GeV. The blue region is the region excluded by LEP results. The red, cyan, and magenta regions correspond to an invisible BR excluded at 75%, 50%, and 25%, respectively.

As an illustration we consider the results from the DELPHI Collaboration [15], where they gave upper bounds for the coefficients $C^2_{Z(H \to b\bar{b})}$ corresponding to a lightest CP-even Higgs boson mass in the range of 15–100 GeV. From this one determines the regions of $m_{H_1} - \sin\alpha$ which are currently allowed by the LEP-II searches. The results are shown in Fig. 1. The region excluded by the LEP results corresponds to the blue regions in this figure. One sees that the LEP results do not exclude much of the parameter space for a light Higgs boson (below 115 GeV) as long as its coupling to the Z boson is reduced with respect to that of the SM. However, in this simple model, if we take into account the discovery at the LHC of a Higgs boson at 125 GeV the parameter space is further restricted. In fact, in this picture the heavier Higgs boson couples to the Z boson with a reduced-strength $\cos\alpha$. The restriction on $\cos\alpha$ depends on the upper limit on the invisible decay of the Higgs boson. Here we consider three values, from 25% up to 75%, which is the current upper bound given by the ATLAS Collaboration [31] for the branching ratio to invisible particle decay modes. This will be improved in the next run of the LHC, but current results indicate that there is still room for such decays, as shown in Fig. 1. Note that the kink in the plot is associated to the decay in Eq. (17).

D. Constraints from visible decay searches

We just saw the implementation of the LHC upper limit on the invisible decay of the Higgs boson. However, we must also enforce the limits coming from the other, well-measured SM channels. These are normally expressed, for an SM final state f, in terms of the signal strength parameter,

$$\mu_f = \frac{\sigma^{\mathrm{NP}}(pp \to h)}{\sigma^{\mathrm{SM}}(pp \to h)} \frac{\Gamma^{\mathrm{NP}}[h \to f]}{\Gamma^{\mathrm{SM}}[h \to f]} \frac{\Gamma^{\mathrm{SM}}[h \to \mathrm{all}]}{\Gamma^{\mathrm{NP}}[h \to \mathrm{all}]}, \quad (22)$$

where σ is the cross section for Higgs production, $\Gamma[h \to f]$ is the decay width into the final state f, the labels NP and SM stand for new physics and Standard Model, respectively, and $\Gamma[h \to \mathrm{all}]$ is the total width of the Higgs boson. These can be compared with those given by the experimental collaborations. We reproduce in Table I the compilation performed in Ref. [32] for the most recent results of the ATLAS [33] and CMS [34] collaborations. One sees that the current limits, although compatible at $1 - \sigma$, still have quite large errors.

Since the number of parameters is very small in our model, it suffices to take as a constraint the limits on μ_{VV} $(V = W, Z)$ in order to illustrate the situation. Instead of taking each experiment individually, we just note that, in a qualitative sense, the LHC results indicate that $\mu_{VV} \sim 1$ to within 20%; that is,

$$0.8 \leq \mu_{VV} \leq 1.2. \quad (23)$$

The results are shown in Fig. 2. In the left panel we consider $v_1 = 1000$ GeV, while in the right panel we let it vary in the range $v_1 \in [500, 1000]$ GeV. As before, the blue region is the LEP exclusion region, while the red region is excluded by the LHC limit on μ_{VV}. The green region is the region still allowed by the current LHC data. If we compare the left panel of Fig. 2 with Fig. 1, which corresponds to the same value of v_1, we see that the limit imposed by μ_{VV} implies, in this model, an upper bound on the invisible Higgs decay of around 20%, which is more stringent that the one presented by the ATLAS Collaboration [31]. This is due to the fact that the number of independent parameters is very much reduced in this model, and the cut on μ_{VV} implies a cut on α. To show this, we plot μ_{ZZ} against $\mathrm{BR}(H_i \to \mathrm{Inv})$ in Fig. 3. The color code is as in Fig. 2. In the left panel we see that the invisible branching ratio of the 125 GeV Higgs boson (H_2 in our model) could be as large as one, but this is ruled out by LEP. Furthermore, the LHC limit on μ_{ZZ} reduces the allowed space, and we obtain an upper bound on the invisible decay for this simple model of around 20%, as we explained before. The corresponding plot for the lightest Higgs boson is shown in the right panel. We see that an

TABLE I. Current experimental results of ATLAS and CMS, taken from the compilation performed in Ref. [32].

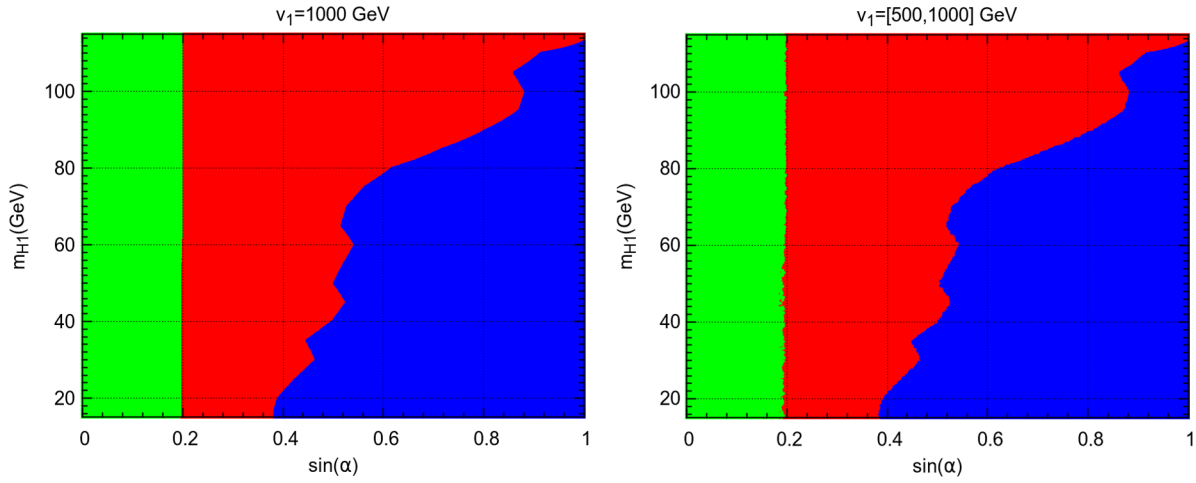| Channel	ATLAS	CMS
$\mu_{\gamma\gamma}$	1.17 ± 0.27	$1.14^{+0.26}_{-0.23}$
μ_{WW}	$1.00^{+0.32}_{-0.29}$	0.83 ± 0.21
μ_{ZZ}	$1.44^{+0.40}_{-0.35}$	1.00 ± 0.29
$\mu_{\tau^+\tau^-}$	$1.4^{+0.5}_{-0.4}$	0.91 ± 0.27
$\mu_{b\bar{b}}$	$0.2^{+0.7}_{-0.6}$	0.93 ± 0.49

FIG. 2 (color online). m_{H_1} versus $\sin\alpha$ in the model for $v_1 = 1000$ GeV (left panel) and $v_1 \in [500, 1000]$ GeV (right panel). The blue region is the region excluded by LEP results. The red region corresponds to the points excluded by the LHC as discussed in the tex,t and the points in the green region pass all constraints.
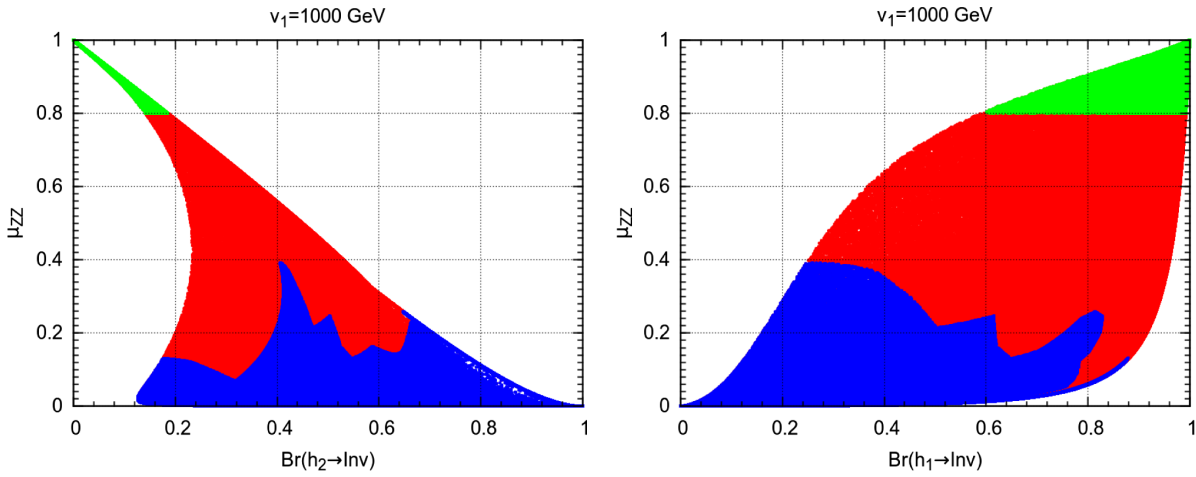

FIG. 3 (color online).   Left panel: μ_{VV} versus $\mathrm{BR}(H_2 \to \mathrm{Inv})$. Right panel: The same for $\mathrm{BR}(H_1 \to \mathrm{Inv})$. The color code is as in Fig. 2.

FIG. 4 (color online).   Left panel: $\mathrm{BR}(H_2 \to \mathrm{Inv})$ as a function of $\mathrm{BR}(H_1 \to \mathrm{Inv})$. Right panel: m_{H_1} as a function of $\mathrm{BR}(H_1 \to \mathrm{Inv})$. The color code is as in Fig. 2.
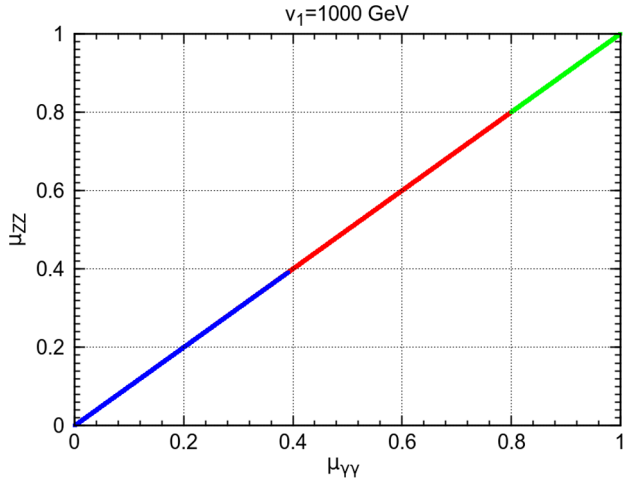
FIG. 5 (color online). Correlation between μ_{ZZ} and $\mu_{\gamma\gamma}$. The color code is as in Fig. 2.

invisible branching ratio of 100% is compatible with the LHC results for this model. The correlation between the invisible branching ratios of the two Higgs bosons is shown in the left panel of Fig. 4 with the same convention for the colors. Finally, in the right panel we plot m_{H_1} as a function of BR($H_1 \to$ Inv), with the same conventions. We see a strong anticorrelation among these panels, due to the simplicity of the model.

In order to better illustrate this anticorrelation, we plot μ_{ZZ} as a function of $\mu_{\gamma\gamma}$ in Fig. 5. The straight line reflects the fact the there is essentially only one parameter left—the angle α—after we fix the two Higgs boson masses. We also notice that in the model, the μ_f for the channels where the final state f exists in the SM can only be less then one. This comes from the reduced coupling of the SM-like Higgs boson.

More general models with a richer Higgs boson sector naturally emerge, for example, in neutrino mass schemes with more than one scalar doublet [8,12,35] or models with a doublet and triplet [36]. In this case, in addition to the scalars considered here there are also charged Higgs bosons. Similar features hold in models where the origin of neutrino mass is supersymmetric, due to spontaneous breaking of R-parity [37,38].

IV. DISCUSSION

In this paper we have given a simple "generic" example illustrating how the physics associated to the Higgs boson may get modified within extensions of the minimal $SU(3)_c \otimes SU(2)_L \otimes U(1)_Y$ theory with spontaneous lepton-number violation at a low scale [6].[3] So far we have

---

[3]High-scale seesaw models may lead to sizable lepton-flavor violation rates coming from supersymmetric contributions [39]. However, here we discard this possibility, since the sizable invisible Higgs boson decay physics would be absent in that case.

considered the simplest scenario for spontaneous breaking of ungauged lepton-number symmetry responsible for inducing the tiny neutrino masses. The latter involves the standard $SU(3)_c \otimes SU(2)_L \otimes U(1)_Y$ electroweak gauge structure, and hence gives rise to a physical Goldstone boson that provides an invisible Higgs decay channel. Such a simple scheme can be implemented in a variety of ways, both at the tree level and within radiative schemes [7,8].

Additional phenomenological signatures beyond the invisible Higgs decay channel in Eq. (1) include charged lepton-flavor violation processes such as radiative muon and tau decays (e.g., $\mu \to e\gamma$, $\mu \to 3e$), as well as mu-e conversion in nuclei. The expected rates for such processes will depend on the details of the model considered. For this reason they have not been discussed explicitly in the present paper. For example, $\mu \to e\gamma$ can be large in inverse seesaw schemes [40–42]. Likewise, mu-e conversion in nuclei is also enhanced [43]. Similar enhancement of lepton-flavor violation processes exists for linear seesaw-type schemes [44]. Similar features arise within radiative models of neutrino mass generation, for example models of the Zee-Babu type [45]. These models also include physical charged scalar bosons running in the neutrino mass loop, and their scalar potential is richer than we have considered above. Note that the charged scalar states present in such models also give a contribution to $H \to \gamma\gamma$ decays. Finally, there is a different class of charged lepton-flavor violation processes involving Majoron emission, for example $\mu \to eJ$. This possibility has been considered, for example, within supersymmetric models with spontaneous R-parity violation [46–48].

V. CONCLUSIONS

Here we have considered the constraints implied by current data, including the Higgs discovery, on the extended electroweak symmetry-breaking potential corresponding to the simplest neutrino mass schemes with spontaneous breaking of lepton number. There are two CP-even Higgs scalars that can decay to Standard Model states as well as invisibly to the Majoron, the pseudoscalar Goldstone boson associated to lepton-number violation. If lepton-number symmetry breaks at the weak scale, the invisible modes can yield potentially large rates for missing-energy events. Using current results from LEP and ATLAS/CMS at the LHC, we have studied the constraints coming from SM searches as well as invisible decays, showing how—despite the large data sample—there is still room for improvement of invisible decay limits in the coming LHC run. Within our simple framework these limits provide a probe into the scale characterizing the violation of lepton number responsible for neutrino mass generation. Having set out the general strategy, other more complex symmetry-breaking sectors may be analyzed in a similar way, such as, for example, those arising in models containing charged Higgs bosons.

[1] G. Aad *et al.* (ATLAS Collaboration), Phys. Lett. B **716**, 1 (2012).

[2] S. Chatrchyan *et al.* (CMS Collaboration), Phys. Lett. B **716**, 30 (2012).

[3] F. Englert and R. Brout, Phys. Rev. Lett. **13**, 321 (1964).

[4] P. W. Higgs, Phys. Lett. **12**, 132 (1964).

[5] P. W. Higgs, Phys. Rev. **145**, 1156 (1966).

[6] J. W. Valle and J. C. Romao, *Neutrinos in high energy and astroparticle physics*, 1st edition (Wiley-VCH, Berlin, 2015).

[7] S. M. Boucenna, S. Morisi, and J. W. Valle, Adv. High Energy Phys. **2014**, 831598 (2014).

[8] A. S. Joshipura and J. Valle, Nucl. Phys. **B397**, 105 (1993).

[9] Y. Chikashige, R. N. Mohapatra, and R. Peccei, Phys. Lett. **98B**, 265 (1981).

[10] J. Schechter and J. Valle, Phys. Rev. D **25**, 774 (1982).

[11] A. S. Joshipura and S. D. Rindani, Phys. Rev. Lett. **69**, 3269 (1992).

[12] J. C. Romao, F. de Campos, and J. W. F. Valle, Phys. Lett. B **292**, 329 (1992).

[13] F. De Campos, J. W. F. Valle, A. Lopez-Fernandez, and J. C. Romao, arXiv:hep-ph/9405382.

[14] F. de Campos, O. J. P. Éboli, J. Rosiek, and J. W. F. Valle, Phys. Rev. D **55**, 1316 (1997).

[15] J. Abdallah *et al.* (DELPHI Collaboration), Eur. Phys. J. C **38**, 1 (2004).

[16] J. Abdallah *et al.* (DELPHI Collaboration), Eur. Phys. J. C **32**, 475 (2004).

[17] R. N. Mohapatra and J. W. F. Valle, Phys. Rev. D **34**, 1642 (1986).

[18] M. C. Gonzalez-Garcia and J. W. F. Valle, Phys. Lett. B **216**, 360 (1989).

[19] E. Akhmedov, M. Lindner, E. Schnapka, and J. W. F. Valle, Phys. Lett. B **368**, 270 (1996).

[20] E. Akhmedov, M. Lindner, E. Schnapka, and J W. F. Valle, Phys. Rev. D **53**, 2752 (1996).

[21] M. Malinsky, J. C. Romao, and J. W. F. Valle, Phys. Rev. Lett. **95**, 161801 (2005).

[22] *Gell-Mann at Stony Brook Supergravity Workshop in 1979, and published in Supergravity*, edited by P. van Nieuwenhuizen and D. Z. Freedman (North Holland Publishing Co, 1979).

[23] T. Yanagida, in *KEK Lectures 1979*, edited by O. Sawada and A. Sugamoto (KEK, Tokyo, 1979).

[24] R. N. Mohapatra and G. Senjanović, Phys. Rev. Lett. **44**, 912 (1980).

[25] J. Schechter and J. Valle, Phys. Rev. D **22**, 2227 (1980).

[26] G. Lazarides, Q. Shafi, and C. Wetterich, Nucl. Phys. **B181**, 287 (1981).

[27] G. Aad *et al.* (ATLAS Collaboration), Phys. Rev. D **90**, 052004 (2014).

[28] V. Khachatryan *et al.* (CMS Collaboration), Eur. Phys. J. C **75**, 212 (2015).

[29] K. Kannike, Eur. Phys. J. C **72**, 2093 (2012).

[30] A. Djouadi, Phys. Rep. **457**, 1 (2008).

[31] G. Aad *et al.* (ATLAS Collaboration), Phys. Rev. Lett. **112**, 201802 (2014).

[32] D. Fontes, J. Romão, and J. P. Silva, J. High Energy Phys. 12 (2014) 043.

[33] G. Aad *et al.* (ATLAS Collaboration), Phys. Rev. D **90**, 112015 (2014).

[34] V. Khachatryan *et al.* (CMS Collaboration), Eur. Phys. J. C **74**, 3076 (2014).

[35] A. Lopez-Fernandez, J. C. Romao, F. de Campos, and J. W. F. Valle, Phys. Lett. B **312**, 240 (1993).

[36] M. A. Diaz, M. Garcia-Jareno, D. A. Restrepo, and J. Valle, Nucl. Phys. **B527**, 44 (1998).

[37] M. Hirsch, J. Romao, J. Valle, and A. Villanova del Moral, Phys. Rev. D **70**, 073012 (2004).

[38] M. Hirsch, J. Romao, J. Valle, and A. Villanova del Moral, Phys. Rev. D **73**, 055007 (2006).

[39] S. Antusch, E. Arganda, M. J. Herrero, and A. M. Teixeira, J. High Energy Phys. 11 (2006) 090.

[40] J. Bernabéu, A. Santamaria, J. Vidal, A. Mendez, and J. W. F. Valle, Phys. Lett. B **187**, 303 (1987).

[41] F. Deppisch and J. W. F. Valle, Phys. Rev. D **72**, 036001 (2005).

[42] P. Dev and R. Mohapatra, Phys. Rev. D **81**, 013001 (2010).

[43] F. Deppisch, T. S. Kosmas, and J. W. F. Valle, Nucl. Phys. **B752**, 80 (2006).

[44] D. Forero, S. Morisi, M. Tortola, and J. W. F. Valle, J. High Energy Phys. 09 (2011) 142.

[45] D. Aristizabal Sierra and M. Hirsch, J. High Energy Phys. 12 (2006) 052.

[46] A. Santamaria and J. W. F. Valle, Phys. Rev. Lett. **60**, 397 (1988).

[47] J. C. Romao, N. Rius, and J. W. F. Valle, Nucl. Phys. **B363**, 369 (1991).

[48] M. Hirsch, A. Vicente, J. Meyer, and W. Porod, Phys. Rev. D **79**, 055023 (2009).